Embrittlement of High Strength β-Ti Alloys

R.P. Gangloff

Department of Materials Science and Engineering, University of Virginia, SEAS-Thornton Hall,
Charlottesville, VA 22903-2442, USA

ABSTRACT

The outstanding strength of α-precipitation hardened β-Ti alloys is compromised by low plane strain fracture toughness, hydrogen embrittlement and perhaps elemental segregation. Solution treated all-β alloys are immune to hydrogen cracking for low to moderate H concentrations, but critical aging to form α triggers transgranular internal hydrogen embrittlement (TG IHE, along α/β interfaces) and intergranular hydrogen environment embrittlement (IG HEE, along β-grain boundaries). Increased strength does not explain this deleterious effect of aging. Rather, the aging dependence of TG IHE appears to be related to H enrichment in β and microscopic stress intensification at α/β interfaces arrayed continuously through β grains. Intergranular HEE is not explained by either grain boundary α formation or deformation localization due to aging. HEE persists when all α is dissolved, suggesting that elemental segregation of Si or impurities may be the requisite for IG cracking, but the offending species have not been resolved.

KEYWORDS

Titanium alloys, fracture toughness, hydrogen embrittlement, fracture mechanics, embrittlement.

INTRODUCTION

Titanium alloys based on a bcc (β) matrix that is hardened by fine precipitates of the hcp-α phase exhibit high strength to weight, excellent formability, and hardenability properties that enable high performance aerospace, marine, and land-based applications [1,2]. For example, a martensitic alloy steel must exhibit a tensile yield strength (σ_{YS}) of about 2400 MPa to exceed the strength-to-density ratio of the strongest β-Ti alloys ($\sigma_{YS} \sim 1600$ MPa). Results suggest, however, that fracture toughness and resistance to hydrogen (H)-assisted cracking are degraded substantially in concert with α strengthening of metastable β. The objective of this work is to examine the effect of α formation on the fracture resistance of modern β/α-Ti alloys, emphasizing deleterious hydrogen embrittlement and the crack tip damage mechanisms that govern damage tolerant properties.

EXPERIMENTAL PROCEDURES

Several β-Ti alloys were examined, including Ti-15-3 (Ti-15V-3Cr-3Sn-3Al in weight pct) [3-5], LCB (Low Cost Beta, Ti-7Mo-4.5Fe-1.5Al) [3], Beta-21S (Ti-15Mo-3Nb-3Al) [4,6], and Beta-C (Ti-8V-6Cr-4Mo-4Zr-3Al) [6-8]. Each alloy contained a total-dissolved H content of $C_H = 25\text{-}200$ ppm (parts-per-million by weight). High strength microstructures were developed by solution treatment (ST) above the β transus, air cooling to retain β only, and heating isothermally to precipitate α. This solution treated and aged (STA) microstructure is shown in Figure 1 for Ti-15-3 sheet where up to 60-volume pct of sub-micrometer α needles precipitate in the Burger's orientation of $\{110\}_\beta \| \{0001\}_\alpha, \langle 111 \rangle_\beta \| \langle 11\bar{2}0 \rangle_\alpha$ [9]. In addition to α, $(Ti,Zr)_5Si_3$ can precipitate at high aging temperatures and ω may be produced at low aging temperatures [9,10].
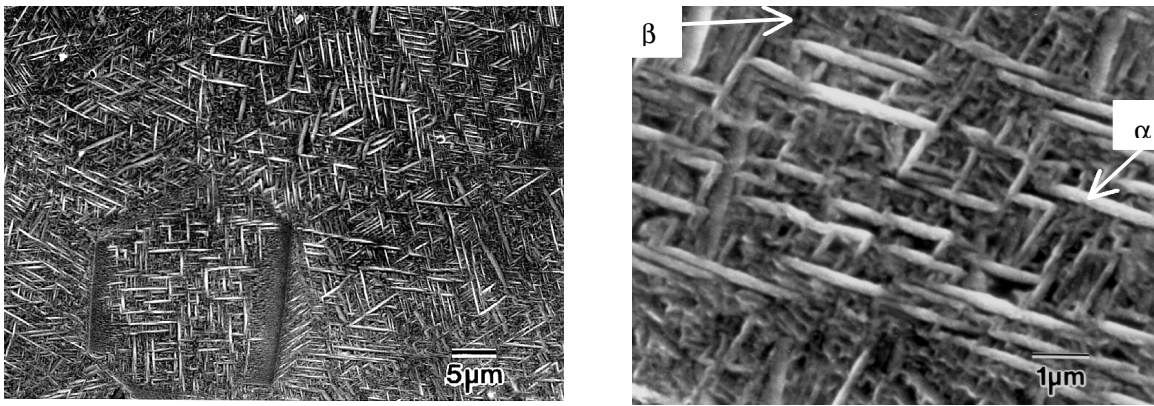
Figure 1: Optical (left) and scanning electron (right) micrographs of the deeply etched microstructure of STA Ti-15-3 sheet showing fine α needles precipitated with long axes that intersect to make angles of 0°, 60° and 90° depending on the sectioning plane and consistent with the Burger's relationship.

Crack growth resistance was measured with a fatigue precracked specimen subjected to increasing crack mouth opening displacement (δ) at a fixed rate and using elastic-plastic J-integral fracture mechanics [11]. For cracking in moist air, the plane strain initiation toughness ($K_{JIC} \sim K_{IC}$ [11]) was obtained for specimens with as-processed levels of H and the threshold K (K_{JTH} or K_{TH}) for the onset of H-assisted subcritical cracking was obtained for specimens electrochemically precharged to C_H of 100 to 10,000 ppm [3]. For specimens in aqueous chloride solution without H precharging, K_{TH} and stable crack growth rate (da/dt) were measured *vs* dK/dt [4,6].

RESULTS AND DISCUSSION

Fracture Toughness
The plane strain fracture toughness of high strength β/α-Ti alloys is deficient compared to martensitic steels at similar high strengths. The data compiled in Figure 2 show that the benefit of the 30% lower density typical of a β-Ti alloy is insufficient to compensate for the very high toughnesses achieved in steels such as AerMet 100 ($K_{IC} \sim 120\text{-}170$ MPa$\sqrt{m}$ at $\sigma_{YS} \sim 1800$ MPa). Such steels exhibit up to an order of magnitude higher fracture toughness compared to K_{IC} approaching 25 MPa$\sqrt{m}$ for very high strength β-Ti alloys.
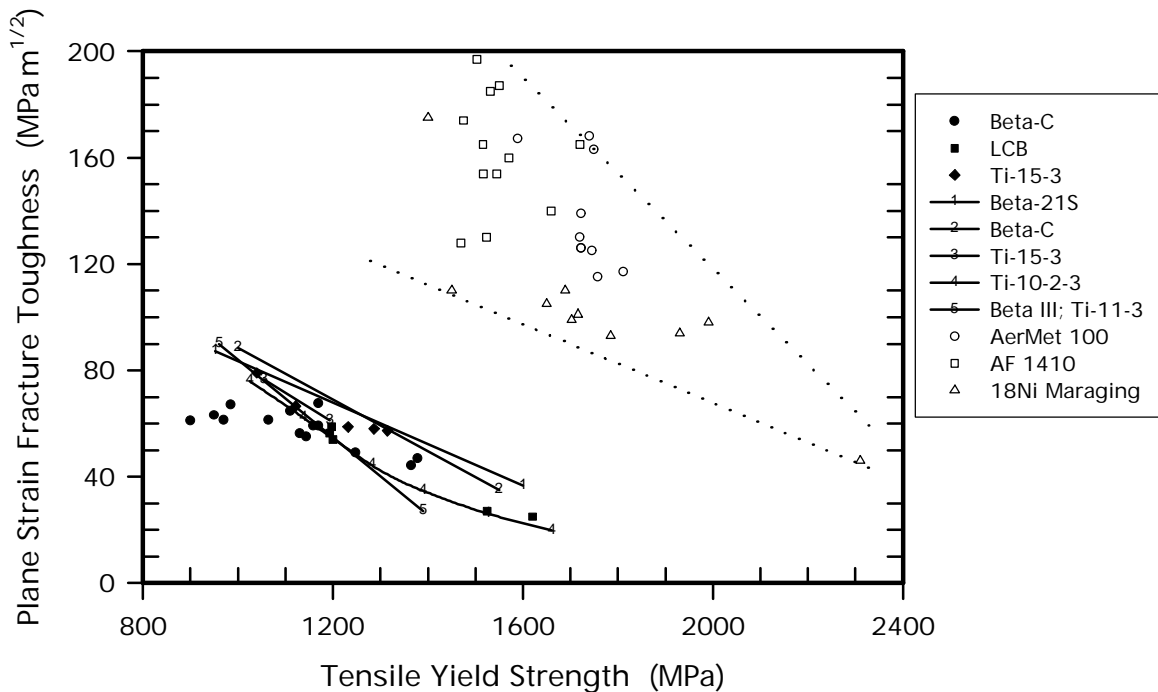

Figure 2: The yield strength dependence of plane strain fracture toughness for a variety of high strength β/α-Ti alloys and martensitic steels fractured in moist air at 25°C.

Low fracture toughness in β-Ti is traced to the size and location of deformable α that localizes plastic strain and tensile stress to exacerbate microvoid nucleation, growth and coalescence [12-16]. For the lower strengths, α films or colonies precipitate heterogeneously at β-grain boundaries and large needles of α precipitate intragranularly; each provides preferred sites for microvoid damage and reduced K_{IC} [3,12,13,15]. To produce high strength, the size of α is reduced and the distribution is homogenized by low temperature aging with added nucleation sites such as dislocations, vacancies, or ω. The toughnesses of such microstructures are, however, low due to deformation banding and microvoid coalescence associated with the particularly high work hardening of fine α relative to β [14-16]. The dependencies of work hardening on α and β size and composition must be better understood, and local stresses from cooperative deformation in α and β must be incorporated into micromechanical models of fracture toughness [17].

Internal Hydrogen Embrittlement

Atomic hydrogen can dissolve in titanium during processing, fabrication, or service to degrade fracture resistance during subsequent deformation, so-called internal hydrogen embrittlement (IHE). Modern STA β/α-Ti alloys are prone to severe IHE for the tensile strengths in Figure 1 [3,5,8,18-20]. For example, experiments with H-precharged STA LCB (σ_{YS} = 1180 MPa) and Ti-15-3 (σ_{YS} = 1200 MPa) sheet showed that K_{TH} for IHE under rising-δ loading (dK/dt = 0.008 MPa√m/s) was reduced to 50% of K_{IC} at C_H levels of 400–500 ppm, and to 25% of K_{IC} at C_H = 750–900 ppm [3]. Absolute values of K_{TH} as low as 12 MPa√m were measured [3].

Aging and/or precipitation of α in β are a requisite for IHE in the moderate-C_H regime (< 2500 ppm) [5,8,18-20]. Figure 3 shows the aging time and strength dependencies of K_{JIC} for as-processed ST Ti-15-3 with 60 ppm H, and K_{JTH} for IHE of ST Ti-15-3 that was H-precharged electrochemically (C_H = 1300 ppm) [3]. ST Ti-15-3 is immune to IHE that only occurs for aging in excess of 5-6 h at 510°C. The reduction in K_{JTH} below K_{JIC} is accompanied by a change from dimpled rupture to transgranular-faceted cracking, as shown in Figure 3. Hydrogen cracking was likely along the interface between α needles and the β matrix, with facet surfaces reflecting the Burger's relationship between α and the multiple variants of {110} in β [3]. Intergranular (IG) cracking was never observed for IHE of STA LCB and Ti-15-3 for conditions typical of the data in Figure 3 [3].
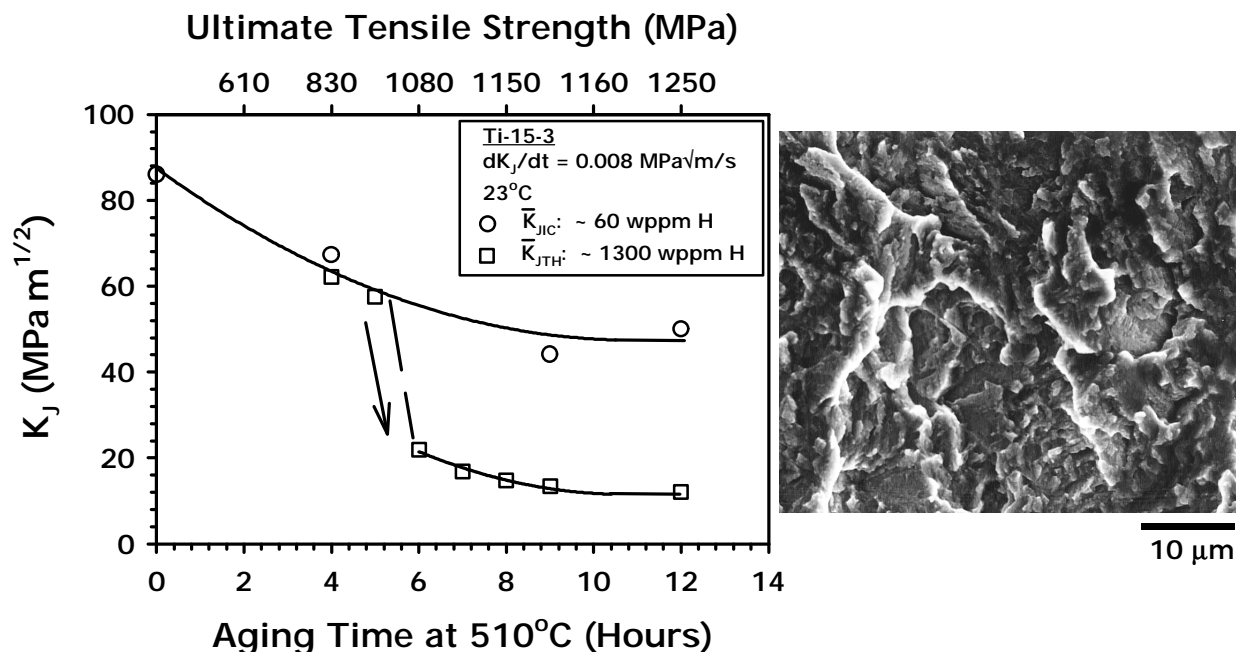

Figure 3: The isothermal-aging time and yield strength dependencies of plane strain fracture toughness at the as-processed H content of 60 ppm and the threshold stress intensity for IHE of H-precharged (C_H = 1300 ppm) ST Ti-15-3 stressed in moist air at 25°C. The SEM fractograph shows the morphology of transgranular IHE for the 12 h age case [3]. (The subscript, J, denotes K calculated from the J-integral and the bar indicates the average of 1st initiation and blunting-line offset definitions of crack growth [3,11].)

Generally, IHE of STA β-Ti alloys involves a variety of fracture modes depending on C_H, α/β microstructure, dK/dt, and constraint. The crack path in STA Beta-C changed from microvoid-based at low C_H, to intergranular along β boundaries (at 1300 ppm H), to crystallographic cleavage (2200 ppm H), to α/β-interface cracking at 3300 ppm H [8,19,20]. Intergranular cracking (1000 ppm H), slip plane cracking (4000 ppm H), and cleavage (5600 ppm H) were associated with IHE in Beta-21S [5,18]. ST β-Ti is susceptible to IHE by cleavage at very high C_H [21].

Hydrogen Environment Embrittlement in Aqueous Chloride Solutions

STA β/α-Ti alloys are susceptible to severe intergranular cracking when stressed in aqueous-NaCl solution [4,6,22-25] and the cracking mechanism was established with substantial certainty to be hydrogen environment embrittlement (HEE) [6,7,26,27]. H is produced exclusively at crack tip sites where the passive film is breached by concurrent plastic deformation and diffuses into the process zone to cause embrittlement. Locally large amounts of H can be introduced into Ti by this electrochemical scenario, provided that an occluded crack tip exists and crack tip strain rate conditions are favorable for H production and uptake [25-29]. Under such conditions, K_{TH} for HEE is as low as 15-20 MPa$\sqrt{m}$ and da/dt is as high as 200 μm/s for STA alloys such as Beta-C and Beta-21S [22-25].

Aging and/or precipitation of α in β is a requisite for IG HEE. Figure 4 shows the strength and isothermal-aging time dependencies of K_{JIC} and K_{TH} for ST Beta-C stressed under rising δ (dK/dt = 0.004 MPa$\sqrt{m}$/s) in moist air and neutral-aqueous chloride solution, respectively [6,22]. ST Beta-C is immune to HEE that only occurs for aging in excess of 3-4 h at 500°C. The reduction in K_{TH} below K_{JIC} is accompanied by a change from microvoid to 100% IG cracking, as shown in Figure 4 and with no evidence of the brittle-transgranular cracking mode typical of IHE (Figure 3).
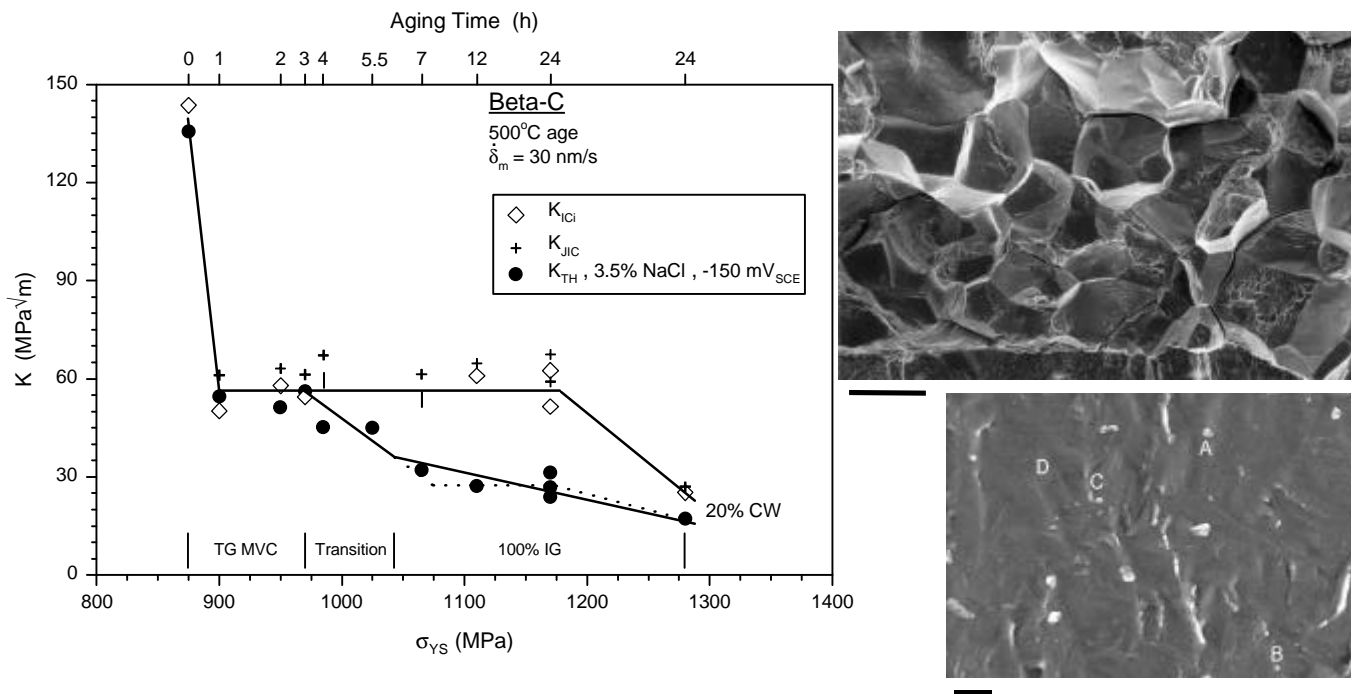

Figure 4: The strength and isothermal-aging time dependencies of fracture toughness and the threshold K for HEE of ST Beta-C stressed in moist air and aqueous-chloride solution at 25°C [6,22]. The highest strength and lowest K_{JIC} were achieved by 20% cold work prior to aging to stimulate fine-α precipitation. SEM fractographs show the morphology of 100% intergranular HEE for the 6 to 24 h age cases (top, 100 μm bar) and the high magnification view of an IG facet surface in these STA microstructures (bottom, 250 nm bar) [36].

Hydrogen Damage Mechanism and Metallurgical Culprit

Both IHE and HEE can be promoted by increasing yield strength since the magnitude of crack tip stresses increases proportionate to 3 to 5 σ_{YS} and H-damage mechanisms are exacerbated [30,31]. However, it is unlikely that strengthening explains the deleterious effect of aging on IHE (Figure 3) and HEE (Figure 4). For Beta-C, the ST β microstructure was immune to HEE for prior cold work levels from 0 to 80 pct, causing strength increases over the range typical of age hardening in Figs. 3 and 4 [22,23]. Experiments with notched-tensile specimens showed that cold worked Beta-C was also immune to IHE [19,20]. Yield strength increases are of secondary importance, perhaps because work hardening decreases with aging to offset the effect of rising σ_{YS}, and blunted crack solutions that equate crack tip stresses to 3-5 σ_{YS} may not be accurate for hydrogen embrittlement due to unique aspects of tip deformation for a crack localized to an interface or grain boundary [32].

Rather than strength, a metallurgical factor that changes during aging is responsible for the occurrence of IHE and HEE in β/α-Ti. Determination of the culprit is complicated by the multiple changes and fine scale of the α microstructure that evolve during aging of ST β-Ti. Additionally, the damage mechanism for hydrogen embrittlement is controversial, with possible contributions from hydride-phase transformation, hydrogen enhanced-localized plasticity, and interface decohesion [30,31,33].

IHE: Considerations of the kinetics of K_{TH} and da/dt *vs* dK/dt for IHE in Ti-15-3 suggest that H diffuses rapidly during loading and over a short distance (0.5-5 μm) through β in the fracture process zone to reach the α/β interface [3]. While brittle TiH may form in α [34], hydrides are less important in β alloys due to the high solubility of H in bcc Ti (~15,000 ppm at 25°C) [19,20]. H is enriched in β when α precipitates are present; local hydriding of α, at the interface with β, should occur for total C_H above 2500 ppm [19,20]. This hydriding was not observed experimentally and is not a likely cause of cracking at the C_H levels in Figure 3. The effect of locally high interface stresses on hydride precipitation is uncertain and this mechanism cannot be discounted. Fracture without H occurs at α/β interfaces in STA alloys such as Ti-15-3. It is reasonable to speculate that this fracture mode is promoted by H, trapped at this interface and with locally high tensile stresses, as envisioned in classic decohesion theory [30,31].

The aging dependence of TG IHE may be understood based on the need for a critical amount of intragranular α. Considering Figure 3, α precipitation was restricted to β-grain boundaries during 0-5 h of aging (α volume fraction of 0 to 0.48) and when Ti-15-3 was immune to IHE. H cracking correlated with α precipitation within many β at the 6 h age (0.52 α) and within all grains at 10-12 h (0.68-0.80 α) [3]. A critical amount of α in β may be required for: (1) a connected path for H cracking [35], (2) locally high tensile stresses from microscopic constraint adjacent to the α/β interface, or (3) H enriched in β and trapped at the interface with α. A connected crack path is not sufficient for IHE since the immune microstructures in Figure 3 exhibited α on all grain boundaries, but IG cracking did not occur.

HEE: Metallurgical variables could promote intergranular HEE by enhancing H production and uptake near β-grain boundaries at the crack tip, and by enabling brittle cracking of H-enriched boundaries within the process zone. Two factors constrain the governing metallurgical variable. The fully-IG fracture mode observed for susceptible STA Beta-C (Figure 4) dictates that the HEE mechanism and variable must operate at essentially every grain boundary, at least for some β-Ti alloys. Second, since H damage appears to occur within 0.1-1 μm of the crack tip surface contacting NaCl solution, the metallurgical variable must be sized and interconnected on this length scale [25,32]. Three microstructural factors may be consistent with these constraints and change during isothermal aging of the ST-β phase: grain boundary α, slip localization, and elemental segregation.

A study isolated these candidate explanations of aging-dependent HEE for the situation represented in Figure 4, but the results were not conclusive [36]. Two features, grain boundary α and H-enhanced slip localization, are not the cause of IG HEE in Beta-C stressed in NaCl solution. TEM and SEM analyses showed that α decorated less than 5% of the β-grain boundaries, but HEE was nearly-100% IG. High magnification examination of matching surfaces of IG facets, using an SEM with a field-emission gun and dual detectors to optimize topographic contrast and resolution, failed to evidence localized plasticity of the sort reported for IG IHE of β/α-Ti [19,20] and hydrogen embrittlement in general [33]. As illustrated by the high-magnification SEM fractograph in Figure 4, the only features resolved were perturbations of the cracked β-grain boundary surface by intersection of occasional α plates. The predominant feature was mildly undulating and featureless grain surfaces, consistent with interface decohesion.

Circumstantial evidence suggested that solute segregation to β-grain boundaries during aging, combined with trapped H, explained the onset of IG HEE in β/α-Ti (Figure 4). A similar explanation was adopted for IG IHE of STA Beta-C [20] and H embrittlement of steels [31]. Results implicated segregated Si as reducing boundary cohesion in β-Ti without H [37]. Experiments, where STA Beta-C was aged at higher temperatures to progressively dissolve α and remove segregation, support the importance of elemental segregation [36]. For example, a double aged and α-free microstructure was susceptible to IG HEE, confirming that grain boundary α and intragranular α are not required for embrittlement. Double aging at higher temperatures and longer times eliminated IG HEE in the all-β microstructure and restored the original ST immunity to cracking. The hypothesis was that HEE was precluded by elimination of boundary segregation, due to either reduced thermodynamic driving force or formation of $(Ti,Zr)_5Si_3$. Boundaries in HEE-immune and susceptible single and double ages of Beta-C were examined by small-probe STEM. No segregant was observed to correlate with the IG cracking tendency. Auger spectroscopy of intergranular facets produced by *in situ* fracture of H-precharged STA Beta-C failed to resolve segregation that correlated with severe IG IHE in long time single-aged specimens [20].

Similar aging times and α precipitation are required to trigger IHE and HEE of ST β-Ti, as shown by the similar K_{TH} relationships in Figures 3 and 4. As such, the mechanisms for these aging dependencies of TG *vs* IG H embrittlement may share a common feature. Elemental segregation to α/β interfaces during aging has not been considered for TG IHE, and enhanced-H trapping from enrichment in β or stress localization due to the presence of α have not been considered for IG HEE.

CONCLUSIONS

1. The outstanding strength capability of α-precipitation hardened β-Ti alloys is compromised by low plane strain fracture toughness compared to martensitic steels, and by both IHE and HEE.
2. All-β alloys are immune to hydrogen embrittlement for low to moderate H concentrations, but transgranular IHE (along α/β interfaces) and intergranular HEE (along β-grain boundaries) are triggered by a critical amount of aging to form α.
3. Increased strength does not explain the deleterious effects of aging on H embrittlement. The onset of TG IHE appears to be related to H enrichment in β and stress intensification at α/β interfaces continuous through β grains. For IG HEE, neither grain boundary α nor deformation localization explain the effect of aging. Segregation may be the requisite for IG cracking, but offending species were not resolved.

REFERENCES

1. Boyer, R.R. and Rosenberg, H.W. (1984). *Beta Titanium Alloys in the 80's*, TMS, Warrendale, PA.
2. Eylon, D., Boyer, R.R. and Koss, D.A. (1993). *Beta Titanium Alloys in the 90's*, TMS, Warrendale, PA.
3. Hayes, S.P. (2000). PhD Dissertation, University of Virginia, Charlottesville, VA.
4. Young, L.M. (1993). MS Thesis, University of Virginia, Charlottesville, VA.
5. Young, G.A. (1993). MS Thesis, University of Virginia, Charlottesville, VA.
6. Somerday, B.P. (1998). PhD Dissertation, University of Virginia, Charlottesville, VA.
7. Kolman, D.G. (1995). PhD Dissertation, University of Virginia, Charlottesville, VA.
8. Gaudett, M.A. (1997). PhD Dissertation, University of Virginia, Charlottesville, VA.
9. Headley, T.J. and Rack, H.J. (1979) *Metall. Trans. A* 10A, 909.
10. Shen, G.Q., Wang, S.H., Liang, T.M., Luo, G.Z. and Xie, L.Y. (1996) *Trans. Metal Heat Treatment* 17, 10.
11. Haynes, M.J. and Gangloff, R.P. (1997) *J. Testing Eval.* 25, 82.
12. Froes, F.H., Chesnutt, J.C., Rhodes, C.G. and Williams, J.C. (1978). In: *Toughness and Fracture Behavior of Titanium, STP 651*, pp. 115-153, ASTM, West Conshohocken, PA.
13. Williams, J.C., Froes, F.H., Chesnutt, J.C., Rhodes, C.G. and Berryman, R.G. (1978). In: *Toughness and Fracture Behavior of Titanium, STP 651*, pp. 64-114, ASTM, West Conshohocken, PA.
14. Terlinde, G.T., Duerig, T.W. and Williams, J.C. (1983) *Metall. Trans. A* 14A, 2101.
15. Terlinde, G.T. and Schwalbe K.-H. (1987). In: *Microstructure, Fracture Toughness and Fatigue Crack Growth in Titanium Alloys*, pp. 97-109, Chakrabarti, A.K. and Chesnutt, J.C. (Eds.). TMS, Warrendale, PA.
16. Terlinde, G.T., Rathjen, H.-J. and Schwalbe K.-H. (1988) *Metall. Trans. A* 19A, 1037.
17. Haynes, M.J. and Gangloff, R.P. (1998) *Metall. Trans. A* 29A, 1599.
18. Young, G.A. and Scully, J.R. (1994) *Corrosion* 50, 919.
19. Gaudett, M.A. and Scully, J.R. (1999) *Metall. Trans. A* 30A, 65.
20. Gaudett, M.A. and Scully, J.R. (2000) *Metall. Trans. A* 31A, 81.
21. Nelson, H.G. (1992). *NASP Government Work Package #92*, NASA Ames Research Center, Moffett Field, CA.
22. Somerday, B.P. and Gangloff, R.P. (1998) *Matls. Sci. Engr. A* A254, 166.
23. Somerday, B.P. and Gangloff, R.P. (1998) *Matls. Sci. Engr. A* A254, 179.
24. Young, L.M., Young, G.A., Scully, J.R. and Gangloff, R.P. (1995) *Metall. Trans. A* 26A, 1257.
25. Somerday, B.P., Young, L.M. and Gangloff, R.P. (2000) *Fatg. Fract. Engr. Matls. Struct.* 23, 39.
26. Kolman, D.G. and Scully, J.R. (1998). In: *Effects of the Environment on the Initiation of Crack Growth, ASTM STP 1298*, pp. 61-73, Van der Sluys, W.A., Piascik, R.S. and Zawierucha, R. (Eds.). ASTM, West Conshohocken, PA.
27. Kolman, D.G. and Scully, J.R. (1997) *Metall. Trans. A* 28A, 2645.
28. Kolman, D.G. and Scully, J.R. (1999) *Phil. Mag. A* 79, 2313.
29. Kolman, D.G., Gaudett, M.A. and Scully, J.R. (1998) *J. Electrochem. Soc.* 145, 1829.
30. Oriani, R.A. (1987) *Corrosion* 43, 390.
31. McMahon, C.J., Jr. (2001) *Engr. Frac. Mech.* 68, 773.
32. Gangloff, R.P. (2001). "Diffusion Control of Hydrogen Environment Embrittlement in High Strength Alloys", In: *Hydrogen Effects on Material Behavior*, Moody, N.R. et al. (Eds.). TMS, Warrendale, PA, in review.
33. Robertson, I.M. (2001) *Engr. Frac. Mech.* 68, 671.
34. Nelson, H.G. (1973) *Metall. Trans. A* 4, 364.
35. Scully, J.R. (2000). In: *Environmentally Assisted Cracking, STP 1401*, pp. 40-69, Kane, R.D. (Ed.). ASTM, West Conshohocken, PA.
36. Somerday, B.P., Wilson, A.W., Howe, J.M. and Gangloff, R.P. (2001) "Microstructural Cause of Intergranular Hydrogen Environment Embrittlement of Aged Beta-Ti Alloys", *Metall. Trans. A,* in review.
37. Graham, D.E. and Koss, D.A. (1978) *Metall. Trans. A* 9A, 1435.